Pathways for N_2 and N_2O Formation during the Reduction of NO_x over Pt−Ba/Al$_2$O$_3$ LNT Catalysts Investigated by Labeling Isotopic Experiments

L. Lietti,* N. Artioli, L. Righini, L. Castoldi, and P. Forzatti

Dipartimento di Energia, Laboratory of Catalysis and Catalytic Processes and NEMAS, Centre of Excellence, Politecnico di Milano, P.zza L. da Vinci 32, Milano, Italy

ABSTRACT: Mechanistic aspects involved in the formation of N_2 and of N_2O during the reduction of gas-phase NO and of NO_x stored over a model PtBa/Al$_2$O$_3$ NSR catalyst are investigated using unlabeled ammonia and labeled NO. The reduction of the stored NO_x species (labeled nitrites and nitrates) with NH$_3$ leads to the selective formation of N_2 as a major product and of small amounts of nitrous oxide. Based on the nitrogen isotopic distribution, it appears that N_2 formation occurs primarily through the statistical coupling of N-atoms formed by dissociation of NO_x- and NH$_3$-related surface intermediates, although an SCR-pathway (involving the coupling of NH$_3$- and NO-derived ad-species) is also likely to occur. It appears as well that the formation of nitrous oxide involves either the coupling of two adsorbed NO molecules or the recombination of an adsorbed NO molecule with an adsorbed NH$_x$ fragment.

■ INTRODUCTION

Both diesel- and lean burn gasoline-powered vehicles are spreading in the transportation sector due to higher efficiency and lower fuel consumption if compared to the traditional stoichiometric engines.[1−3] The three-way-catalytic (TWC) converters, currently used for stoichiometric gasoline engines, are not effective in the reduction of NO_x for lean burn engines, which operate in the presence of excess oxygen. Viable solutions for the control of NO_x are in these cases the urea-SCR technique and the NO_x storage reduction (NSR) or lean NO_x trap (LNT) system.[4−6] To date, the urea-SCR technology is preferred for heavy-duty vehicles and minivans, whereas LNTs are preferred for small engines.[7] Besides, hybrid LNT/SCR systems have also been proposed.[1,8]

In the NSR technology long lean phases, typically lasting 60−90 s, during which NO_x are stored on the catalyst, are alternated with short rich periods, in the order of few seconds, where the exhaust is deliberately made rich. The trapped NO_x are reduced to N_2 although other byproduct may be released (NO, N_2O, NH$_3$). NSR catalysts are composed of a high surface area support material (often γ-alumina or stabilized alumina), precious metals (usually a combination of Pt and Rh), and basic components, such as Ba or K, which act as NO_x storage material.[9,10]

Mechanistic aspects of the reduction of NO_x stored over NSR catalytic systems have been investigated by several groups.[11−15] It has been shown that the reduction of stored nitrates by hydrogen under nearly isothermal conditions (i.e., in the absence of significant thermal effects upon the lean/rich switch) does not involve the thermal decomposition of the adsorbed NO_x species as a preliminary step,[11,16] but instead occurs via a Pt-catalyzed route already active at low temperatures. Besides, it has been suggested that N_2 is formed through a two-steps process in series molecular pathway involving the fast reaction of nitrates with hydrogen to give ammonia, followed by the slower reaction of the so-formed NH$_3$ with residual stored nitrates to

give N_2.[13,14,17,18,21] Owing to the high reactivity of H_2 toward nitrates, and to the integral nature of the reactor, an hydrogen front develops in the reactor so that NH$_3$ reacts with nitrates stored downstream from the H_2 front to give nitrogen. This has been clearly demonstrated by spaciMS measurements[19] showing the intracatalyst spatiotemporal species distributions during regeneration with H_2 of a Pt−Ba/Al$_2$O$_3$ LNT trap. As also pointed out by a dedicated kinetic analysis,[20] the development of an H_2 front traveling in the reactor, along with the occurrence of the above two-steps in series pathway, is able to account for the temporal sequence of products observed at the reactor exit during the regeneration of NSR catalysts.[15,14,21]

On the basis of these findings, it appears that N_2 formation during the regeneration of NSR catalysts occurs via the reaction of ammonia with stored NO_x. Mechanistic aspects of this reaction are still largely unclear: this has motivated the present study where the possible routes leading to the formation of N_2 during the reaction of NH$_3$ with the stored NO_x have been investigated. For this purpose, isotopic labeling experiments have been carried out using unlabeled NH$_3$ and ^{15}NO as a source for the stored $^{15}NO_x$. Since nitrites and nitrates can be formed on the catalyst surface upon NO adsorption in the presence of O_2 at low and high temperature, respectively,[25,26] the reactivity of these adsorbed species with gaseous NH$_3$ has been investigated. The reactivity of NH$_3$ and ^{15}NO in the gas phase has also been studied for comparison purposes. This allowed better clarification of the mechanistic aspects involved in the formation of N_2 during regeneration of the NSR catalysts, as detailed below.

■ MATERIALS AND METHODS

Catalysts Preparation and Characterization. A homemade Pt−Ba/Al$_2$O$_3$ (1/20/100 w/w) catalyst was used in this study. The catalytic system was prepared by incipient wetness impregnation of a commercial alumina sample (Versal 250 from UOP) with an aqueous solution of dinitro-diammine platinum (Strem Chemicals, 5% Pt in ammonium hydroxide) and subsequently with a solution of Ba acetate (Aldrich, 99%). The powder was dried at 80 °C and calcined in air at 500 °C for 5 h after each impregnation step.[22] The impregnation order (first Pt and then Ba) was chosen in order to ensure a good dispersion and stability of the noble metal and of the alkaline component on the alumina support, in line with recipes of Toyota patents.[23]

The specific surface area of the sample, determined by N$_2$ adsorption−desorption using a Micromeritics TriStar 3000 instrument, is 160 m^2 g^{-1} (BET method). The Pt dispersion was also estimated by hydrogen chemisorption at 0 °C (TPD/R/O 1100 Thermo Fischer instrument); a value of 52% was obtained.

Catalytic Tests. Catalytic tests were performed in a quartz tube microreactor (7 mm I.D.) loaded with 60 mg of catalyst powder (70−100 μm). A total flow of 100 cm^3/min (at 1 atm and 0 °C) was used in the experiments, resulting in a GHSV of 10^5 h^{-1}, the density of the catalyst bed being very close to 1 g/cm^3. The reactor outlet was directly connected to a mass spectrometer (Thermostar 200, Pfeiffer), a UV-NO$_x$ analyzer (LIMAS 11HW, ABB) and a microgas chromatograph (Agilent 3000A) for online analysis of the reaction products.[16,22,24]

Prior to the catalytic activity runs, the catalyst sample was conditioned by performing a few storage/regeneration cycles. For this purpose NO$_x$ was adsorbed at 350 °C by imposing a rectangular step feed of NO (1000 ppm) in flowing He + 3% v/v O$_2$ until catalyst saturation. Then the NO and O$_2$ concentrations were stepwise decreased to zero, followed by a He purge at the same temperature (350 °C). This leads to the desorption of weakly adsorbed NO$_x$ species. After the He purge, catalyst regeneration (rich phase) was carried out with H$_2$ (2000 ppm in He). Conditioning lasted until a reproducible behavior was obtained; this typically required 3−4 adsorption/reduction cycles. The conditioning procedure terminated with a reducing step; accordingly before the subsequent experiments the catalyst surface was free of any adsorbed NO$_x$ species.

After the catalyst was conditioned at 350 °C, the temperature-programmed reaction (TPR) of NH$_3$ + ^{15}NO, and temperature programmed surface reaction (TPSR)/isothermal step concentration (ISC) experiments of nitrites and nitrates with ammonia were performed. In a typical TPR experiment, the catalyst was exposed under temperature programming from room temperature (RT) to 400 °C (10 °C/min) to a flow of 660 ppm of NH$_3$ and 1000 ppm ^{15}NO in He (i.e., according to the stoichiometry of the slow SCR reaction: 6NO + 4NH$_3$ → 5N$_2$ + 6H$_2$O).

Before TPSR and ISC experiments, labeled nitrites and nitrates have been adsorbed on the catalyst surface. On the basis of previous NO$_x$ adsorption studies under in situ and operando conditions, nitrite and nitrate ad-species are formed on the catalyst surface upon NO/O$_2$ adsorption at low (150 °C) and high (350 °C) temperature, respectively.[25−27] Accordingly labeled nitrites and nitrates were accumulated by contacting the catalyst with a flow of 1000 ppm ^{15}NO in He + 3% v/v O$_2$ at 150 and 350 °C, respectively.

In the case of TPSR experiments, after ^{15}NO$_x$ adsorption followed by a He purge at the same temperature, the catalyst was cooled down to RT under He flow. Then a rectangular step feed of NH$_3$ (1000 ppm in He) was admitted to the reactor at RT and the catalyst temperature was linearly increased to 400 °C (heating rate 10 °C/min, hold 1 h), while monitoring the concentration of the products exiting the reactor. This procedure led to complete removal of the stored ^{15}NO$_x$, as confirmed by nitrogen balance.

In the case of the isothermal step concentration experiments (ISC), after ^{15}NO$_x$ adsorption and He purge at 150 or 350 °C, the reduction of the stored ^{15}NO$_x$ species was carried out at the same temperature by imposing a rectangular step feed of NH$_3$ (1000 ppm in He).

At the end of the regeneration procedure, the catalyst was heated up to 350 °C under He flow and eventually hydrogen was added to the reactor to complete the reduction of residual stored ^{15}NO$_x$, if any. This procedure allowed the quantification of the residual ^{15}NO$_x$ species left after reduction.

The following mass-to-charge ratios (m/e) have been used to follow the reaction products: H$_2$ (m/e = 2), N$_2$ (m/e = 28), ^{15}NN (m/e = 29), ^{15}N$_2$ (m/e = 30), NO (m/e = 30), ^{15}NO (m/e = 31), N$_2$O (m/e = 44), ^{15}NNO (m/e = 45), ^{15}N$_2$O (m/e = 46), H$_2$O (m/e = 18), NH$_3$ (m/e = 15), NO$_2$ (m/e = 46), ^{15}NO$_2$ (m/e = 47), and ^{15}NH$_3$ (m/e = 16). Because of the large overlapping of the cracking patterns of the reaction products, quantitative analysis has been accomplished by simultaneous mass spectrometry, gas-chromatography, and UV−vis analysis.

Calibration factors and cracking patterns of the unlabeled species have been experimentally determined from calibrated gas cylinders; those of several labeled species have been obtained from cylinders (^{15}NO) or by dedicated experiments (e.g., lean rich cycles with ^{15}NO leading to the formation of ^{15}NO$_2$, ^{15}N$_2$, and ^{15}NH$_3$). This procedure revealed that the calibration factors of ^{15}N$_2$ and N$_2$ were almost identical; accordingly that of ^{15}NN was assumed to be the same. Along similar lines the calibration factors of ^{15}N$_2$O and ^{15}NNO were assumed to be identical to that of N$_2$O. These results have also been confirmed by GC measurements.

The analytical setup used in this work allowed the identification and quantification of species which overlap each other. For example the ^{15}N$_2$ concentration was obtained from the MS m/e = 30 signal after "cleaning" the NO and NH$_3$ contributions provided by simultaneous UV−vis analysis; the ^{15}NH$_3$ concentration was estimated by subtracting from the total amount of ammonia (NH$_3$ + ^{15}NH$_3$) obtained from the UV analyzer the concentration of ^{14}NH$_3$ obtained from the MS signal at m/e = 15 (taking into account the overlapping of ^{15}N). Besides, GC analysis allowed the quantification of the overall nitrogen (N$_2$ + ^{15}NN + ^{15}N$_2$) and nitrous oxide (N$_2$O + ^{15}NNO + ^{15}N$_2$O) concentrations at different instants of the runs. These total concentration values were compared to those calculated by the sum of the different isotopic species (^{15}N$_2$ + N$_2$ + ^{15}NN and ^{15}N$_2$O + N$_2$O + ^{15}NNO) measured with the mass spectrometer to verify the accuracy of the analysis method.

N-balances, calculated from the amounts of NO$_x$ adsorbed and those of N-containing products, are generally within an experimental error of 10%.

All the experiments carried out with ^{15}NO (TPSR and ISC) have been performed with ^{14}NO as well to check for differences in the reactivity of the labeled and unlabeled molecules: differences have always been found to be negligible.

■ RESULTS

Adsorption of Nitrites and Nitrates. On the basis of previous NO_x adsorption studies accomplished under in situ and operando conditions[25−27] nitrite and nitrate ad-species are formed on the Pt−Ba/Al$_2$O$_3$ catalyst surface upon NO/O$_2$ adsorption at low (150 °C) and high (350 °C) temperature, respectively. The results of ^{15}NO/O$_2$ storage are shown in Figure 1 panels A and B. In Figure 1A ($T = 150$ °C) the ^{15}NO
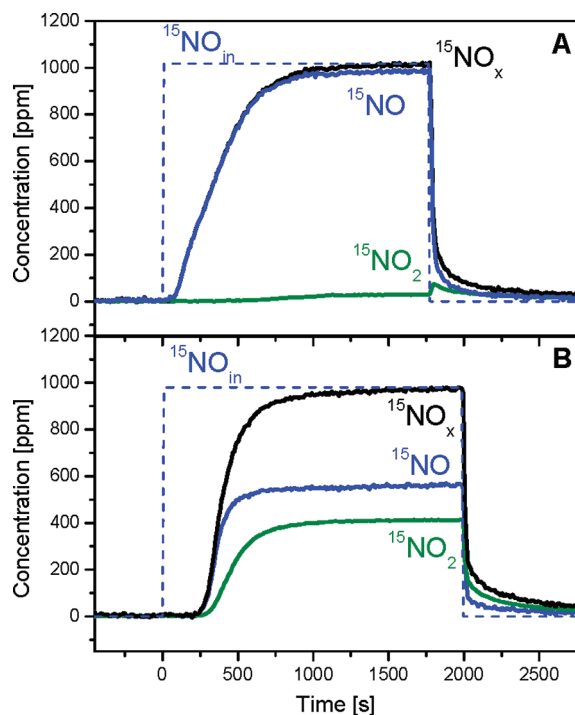

Figure 1. Adsorption of labeled NO at (A) 150 and (B) 350 °C by imposing a rectangular step feed of ^{15}NO (1000 ppm) in flowing He + 3% v/v O$_2$ on Pt−Ba/Al$_2$O$_3$ catalyst.

breakthrough is immediately observed upon admission ($t = 0$ s), along with very small amounts of ^{15}NO$_2$ which are seen after 500 s. After steady-state conditions are attained, the ^{15}NO inlet concentration is switched to zero; a tail is observed in the NO$_x$ outlet concentration (with a small "puff" in the NO$_2$ concentration) due to the desorption of weakly adsorbed species. At the end of the adsorption process (2750 s), nearly 0.26 mmol/g$_{cat}$ of ^{15}NO$_x$ have been stored on the catalyst surface.

In Figure 1B ($T = 350$ °C) the ^{15}NO breakthrough is observed at 200 s, and the evolution of significant amounts of ^{15}NO$_2$ are observed starting from 260 s. The outlet concentrations of both ^{15}NO and ^{15}NO$_2$ increase with time and tend to constant levels which are consistent with the constraints of the equilibrium of ^{15}NO oxidation to ^{15}NO$_2$ in the presence of 3% v/v O$_2$ (^{15}NO = 590 ppm vs ^{15}NO$_{eq}$ = 445 ppm and ^{15}NO$_2$ = 410 ppm vs ^{15}NO$_{2eq}$ = 555 ppm, at 350 °C). After roughly 2000 s, the ^{15}NO feed is switched off, and also in this case a tail is observed in the ^{15}NO$_x$ concentration profile, due to the desorption of the weakly adsorbed ^{15}NO$_x$ species. At the end of the storage phase, nearly 0.34 mmol/g$_{cat}$ of ^{15}NO$_x$ have been stored on the catalyst surface.

Reactivity of Stored Nitrites and Nitrates with Gas-Phase NH$_3$. Figures 2 and 3 show the results of NH$_3$-TPSR and NH$_3$-ISC experiments carried out after ^{15}NO$_x$ storage at 150 °C (labeled nitrites).
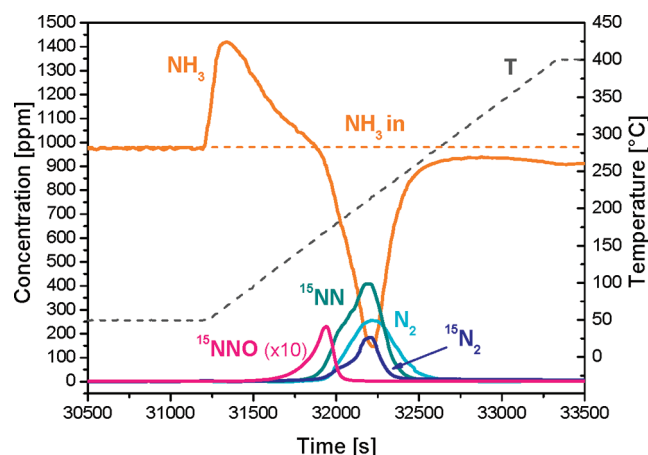

Figure 2. TPSR run with NH$_3$ (1000 ppm) after ^{15}NO$_x$ adsorption at 150 °C (1000 ppm ^{15}NO + O$_2$ 3% v/v in He) over Pt−Ba/Al$_2$O$_3$ catalyst.

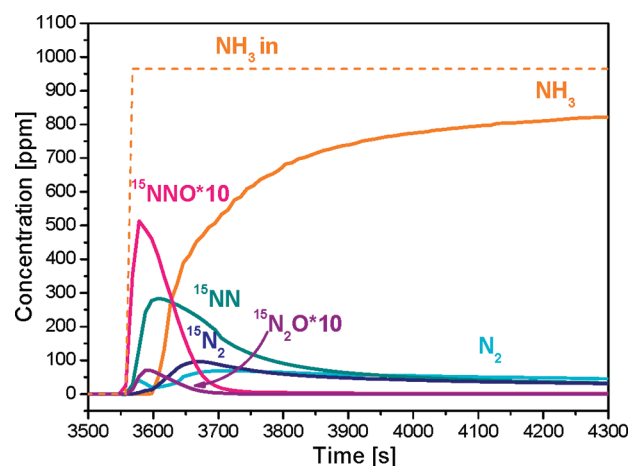**Figure 3.** ISC-rich phase with NH$_3$ (1000 ppm) at 150 °C after ^{15}NO$_x$ adsorption at 150 °C (1000 ppm ^{15}NO + O$_2$ 3% v/v in He) over Pt−Ba/Al$_2$O$_3$ catalyst.

In the case of the TPSR experiment (Figure 2), the desorption of ammonia is observed at first; indeed ammonia is being stored on the catalyst upon admission at the beginning of the experiment, not shown in the Figure ($t < 30500$ s). From nearly 120 °C a net consumption of ammonia is seen together with the formation of N$_2$O and N$_2$ due to the reaction of NH$_3$ with stored ^{15}NO$_x$. Nitrogen is by far the most abundant product, with different isotopic composition. The single-labeled isotope (i.e., ^{15}N^{14}N, $m/z = 29$) is initially observed in greater amounts, whereas the unlabeled (^{14}N$_2$, $m/z = 28$) and double-labeled (^{15}N$_2$, $m/z = 30$) species are seen with a short delay. The single-labeled ^{15}N^{14}N molecule is the most abundant dinitrogen species evolved during the experiment (49% of the total N$_2$ products), but the unlabeled (^{14}N$_2$) and double-labeled (^{15}N$_2$) dinitrogen are also observed in significant amounts (35% and 16%, respectively). The evolution of very small amounts of single-labeled nitrous oxide (^{15}N^{14}NO, $m/z = 47$) is also observed at the onset of the reaction around 100 °C (note that the concentration trace of ^{15}N^{14}NO is multiplied by a factor of 10).

Notably, the NH$_3$ consumption (0.3 mmol/g$_{cat}$, as estimated from the NH$_3$ uptake in Figure 2 in the temperature range

120−300 °C) and the N_2 formation (0.29 mmol/g_{cat}) roughly obey the stoichiometry of reaction 1:

$$Ba(NO_2)_2 + 2NH_3 \rightarrow 2N_2 + BaO + 3H_2O \qquad (1)$$
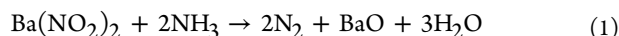
Indeed nitrites are formed upon storage of NO/O_2 at 150 °C, and N_2 represents the major reaction product of NH_3-TPSR.[25,26] Above 300 °C, ammonia is decomposed to a small extent into N_2 and H_2 (these species can be hardly detected due to the low concentrations).

Figure 3 shows the results obtained upon reduction of the stored nitrites at 150 °C (NH_3-ISC). Upon admission, ammonia is completely consumed and nitrogen is formed as the major reaction product along with nitrous oxide in small amounts (its concentration trace is multiplied by a factor of 10). The NH_3 consumption is slightly higher than that expected from the stoichiometry of reaction 1 due to ammonia adsorption onto the catalyst surface.

The temporal sequence and the distribution of products resemble those seen during the TPSR run (Figure 2). The single-labeled $^{15}N^{14}N$ molecule represents the main dinitrogen isotopic product (53%) and is seen before the other isotopes; $^{14}N_2$ and $^{15}N_2$ account for 23% and 24% of total N_2, respectively. Concerning N_2O, the single-labeled molecule ($^{15}N^{14}NO$) is formed in significant amounts, along with traces (few ppm) of the double-labeled isotope ($^{15}N_2O$). The unlabeled molecule $^{14}N_2O$ is not observed.

The results obtained upon the reaction of ammonia with the stored nitrates are shown in Figures 4 and 5. In the case of the
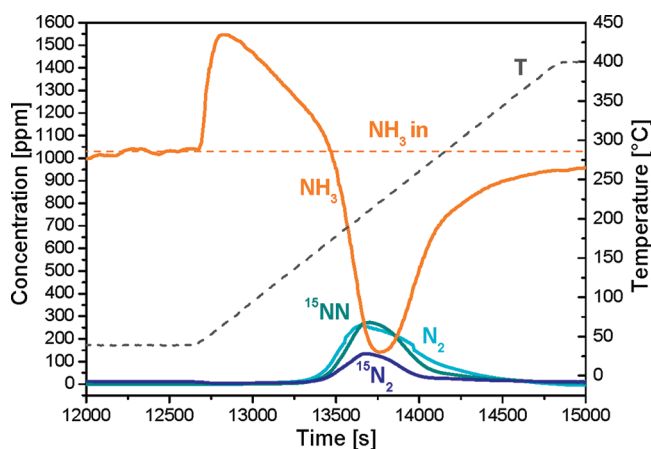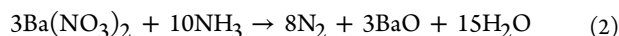

Figure 4. TPSR run with NH_3 (1000 ppm) after $^{15}NO_x$ adsorption at 350 °C (1000 ppm ^{15}NO + O_2 3% v/v in He) over Pt−Ba/Al$_2$O$_3$ catalyst.

NH_3-TPSR experiment (Figure 4), the ammonia consumption is observed from near 150 °C, and is accompanied by the evolution of N_2. The consumption of ammonia (0.6 mmol/g_{cat}) and the formation of N_2 (0.5 mmol/g_{cat}) are in line with the stoichiometry of reaction 2:

$$3Ba(NO_3)_2 + 10NH_3 \rightarrow 8N_2 + 3BaO + 15H_2O \qquad (2)$$

Indeed nitrates are formed upon storage of NO/O_2 at 350 °C and N_2 represents the only reaction product in Figure 4. N_2O is not observed in this case, at variance with the NH_3-TPSR of nitrites (Figure 2) and in line with previous literature reports showing that the reduction of nitrates with ammonia is very selective toward N_2.[13,14,17,18] The dynamics of the evolution of the three dinitrogen isotopes is the same; the unlabeled
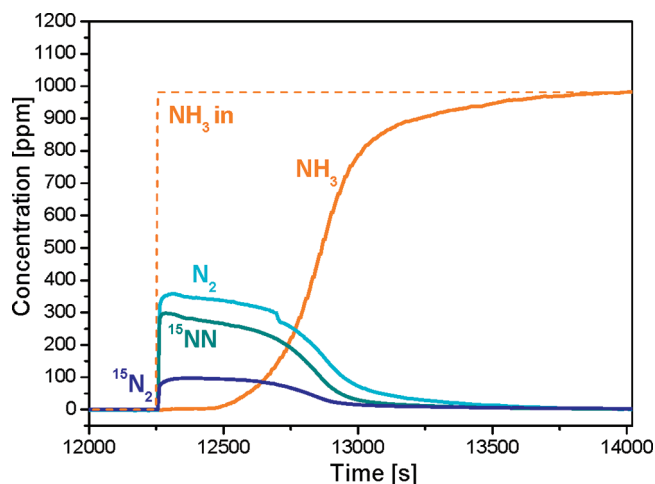

Figure 5. ISC-rich phase with NH_3 (1000 ppm) at 350 °C after $^{15}NO_x$ adsorption at 350 °C (1000 ppm ^{15}NO + O_2 3% v/v in He) over Pt−Ba/Al$_2$O$_3$ catalyst.

$^{14}N_2$ and the single-labeled $^{15}N^{14}N$ species are most abundant (respectively 44% and 37%), while $^{15}N_2$ accounts for 19% of total N_2.

Similar results have been obtained in the case of NH_3-ISC carried out over the stored nitrates at 350 °C (Figure 5). Ammonia is completely consumed upon admission and N_2 represents the only reaction product. At 350 °C the adsorption of ammonia is negligible, so that the consumption of ammonia and the formation of N_2 obey the stoichiometry of reaction 2, as opposite to what was observed in the case of nitrites where the NH_3-ISC experiment was carried out at much lower temperature (150 °C, Figure 3). Unlabeled $^{14}N_2$ and single-labeled $^{15}N^{14}N$ species represent the main products (50% and 35%, respectively), while lower amounts of $^{15}N_2$ are observed (15%). As in the case of NH_3-TPSR of nitrates (Figure 4), N_2O is not observed, and the reaction is fully selective toward nitrogen.

Reactivity of Gas-Phase NO and NH_3. The results of TPR of NH_3 with gas-phase ^{15}NO are shown in Figure 6. The
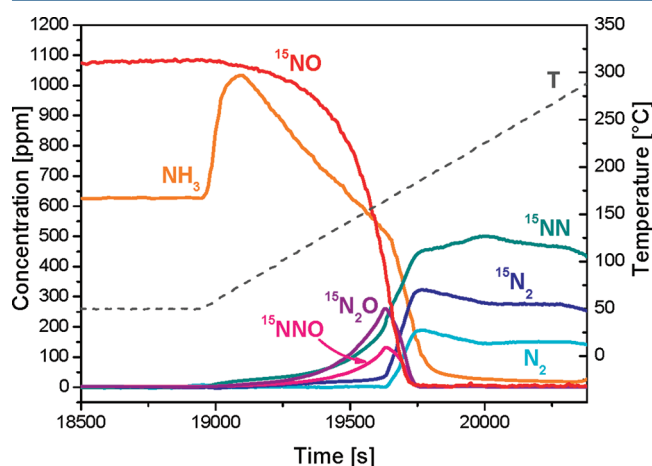

Figure 6. TPR run with NH_3 (660 ppm) and ^{15}NO (1000 ppm) in He over Pt−Ba/Al$_2$O$_3$ catalyst.

onset of the reaction with formation of N_2O and N_2 in comparable amounts is observed at 100 °C. Up to 180 °C only labeled molecules are detected, that is, $^{15}N_2O$ and $^{15}N^{14}NO$ for nitrous oxide and $^{15}N^{14}N$ for dinitrogen. Above 180 °C, where

complete NO consumption is observed, the concentration of nitrous oxide species drops to zero and the formation of double-labeled $^{15}N_2$ and of unlabeled $^{14}N_2$ is observed. Hence above 180 °C the reaction is very selective toward N_2.

■ DISCUSSION

Mechanism of N_2 Formation. The results show that the NO_x species stored onto $PtBa/Al_2O_3$ LNT catalyst, i.e. nitrites and nitrates, are selectively reduced by NH_3 to N_2, since no other products are observed if one neglects the formation of very small amounts of nitrous oxide in the reduction of nitrites. All dinitrogen isotopes are formed but the abundance of the single-labeled $^{15}N^{14}N$ isotope is greater than those of the unlabeled $^{14}N_2$ and double-labeled $^{15}N_2$ isotopes. Only in the case of nitrites the dinitrogen isotopes show different temporal evolution; indeed the single-labeled $^{15}N^{14}N$ isotope prevails at the beginning of both NH_3-TPSR and NH_3-ISC runs. Concerning nitrous oxide, only labeled species ($^{15}N^{14}NO$ and $^{15}N_2O$) are formed upon reaction of the stored NO_x with ammonia.

A different picture is apparent in the reaction of ammonia with gaseous ^{15}NO. In this case comparable amounts of N_2O and of N_2 are observed at low temperature (100−180 °C), but the selectivity to dinitrogen is complete above 180−200 °C where NO is completely consumed. Like during NH_3-TPSR and NH_3−ISC runs of both nitrites and nitrates, only labeled species are observed in the case of nitrous oxide ($^{15}N^{14}NO$ and $^{15}N_2O$). On the other hand all types of dinitrogen isotopes are observed among the products, but only the single-labeled $^{15}N^{14}N$ isotope is detected at 100−180 °C.

Mechanistic aspects involved in the formation of dinitrogen during the reduction of NO_x by NH_3 have been the object of long debate in the scientific literature. In the case of the NH_3−SCR reaction over vanadia-based catalysts and transition metal exchanged zeolites

$$4NO + 4NH_3 + O_2 \rightarrow 4N_2 + 6H_2O \qquad (3)$$
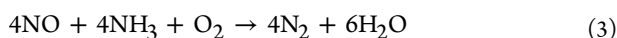
it has been shown that the reaction between unlabeled ammonia ($^{14}NH_3$) and labeled NO (^{15}NO) leads to the selective formation of the single-labeled nitrogen molecule ($^{15}N^{14}N$),[28−30] indicating that one N-atom comes from ammonia and the other from NO. Accordingly the formation of N_2 has been suggested to occur through the intermediacy of surface species like nitrosamide or ammonium nitrite[29,31,32,29] formed via coupling of NH_3- with NO-derived species. In this pathway (SCR pathway) the self-coupling of N-species that originated from ammonia and NO is ruled out because of the lack of significant amounts of $^{15}N_2$ and $^{14}N_2$ isotopes in the product mixture. The same conclusions have been reached in our laboratories where the reaction of stored $^{14}NH_3$ with ^{15}NO in the presence of excess O_2 has been accomplished over V_2O_5/TiO_2 and Fe-ZSM5 catalyst samples. In fact the very selective formation of $^{14}N^{15}N$ was observed (data not reported for the sake of brevity), in line with previous literature reports and with the mechanistic indications discussed above.[28,30]

A different picture is apparent in the reduction of NO_x with ammonia in the case of the $PtBa/Al_2O_3$ catalyst sample investigated in this work. In the reduction of stored labeled nitrites by $^{14}NH_3$ (Figures 2 and 3) the formation of all dinitrogen isotopes was observed. The single-labeled $^{14}N^{15}N$ species dominates (roughly 50% of total N_2), but relevant amounts of double-labeled ($^{15}N_2$) and unlabeled ($^{14}N_2$) dinitrogen are also observed.

It is worth noting that the stoichiometry of the reduction of stored nitrites with ammonia (reaction 1) involves, like the NH_3−SCR reaction 3, a 1/1 molar ratio between $^{14}NH_3$ and the nitrite group $^{15}NO_2{}^-$. Accordingly in this case the selective formation of only the single-labeled $^{14}N^{15}N$ molecule (via coupling of ^{14}N- and ^{15}N-containing species, as in the case of the SCR pathway) is possible. However the production of $^{15}N_2$ and unlabeled $^{14}N_2$ has also been observed, in addition to $^{14}N^{15}N$, and this indicates that a SCR-like pathway does not represent the unique route of N_2 formation in the case of LNT catalysts.

Figure 7 sketches a possible pathway that can explain the formation of dinitrogen (and of nitrous oxide, see below)
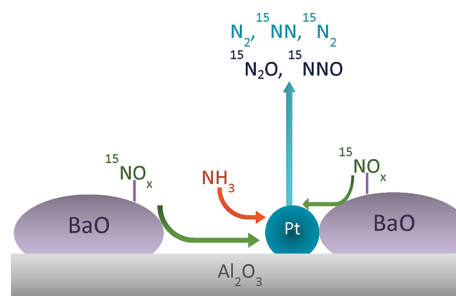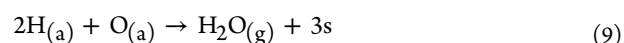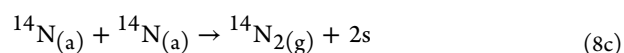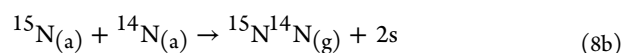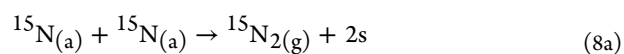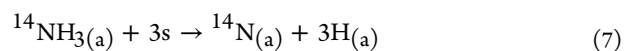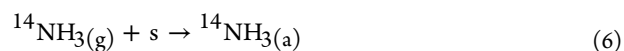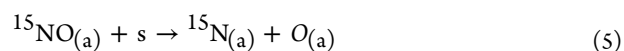

Figure 7. Reaction pathway for $^{15}NO_x$ reduction over Pt−Ba/Al_2O_3 catalyst.

during the reduction by NH_3 of $^{15}NO_x$ adsorbed over Pt−Ba/Al_2O_3. Stored $^{15}NO_x$ are located on Ba sites close to or far away from Pt; upon admission of ammonia the Pt sites are reduced and this drives the onset of the reduction process which involves the migration through surface diffusion of stored $^{15}NO_x$ toward reduced Pt sites, as suggested in the literature.[33] The $^{15}NO_x$ species are hence decomposed at the reduced Pt sites with formation of a pool of ^{15}N- and O- ad-atoms. These ad-species react with NH_3-derived species or fragments adsorbed onto the Pt sites, as suggested in the case of the NO-NH_3 reaction over Pt-based catalysts.[6,12,34−38] In such a case there is a general consensus that dinitrogen formation occurs via recombination of N-ad-atoms formed by dissociation of NO and NH_3 at the Pt site (s):

$$^{15}NO_{(g)} + s \rightarrow {}^{15}NO_{(a)} \qquad (4)$$

$$^{15}NO_{(a)} + s \rightarrow {}^{15}N_{(a)} + O_{(a)} \qquad (5)$$

$$^{14}NH_{3(g)} + s \rightarrow {}^{14}NH_{3(a)} \qquad (6)$$

$$^{14}NH_{3(a)} + 3s \rightarrow {}^{14}N_{(a)} + 3H_{(a)} \qquad (7)$$

$$^{15}N_{(a)} + {}^{15}N_{(a)} \rightarrow {}^{15}N_{2(g)} + 2s \qquad (8a)$$

$$^{15}N_{(a)} + {}^{14}N_{(a)} \rightarrow {}^{15}N^{14}N_{(g)} + 2s \qquad (8b)$$

$$^{14}N_{(a)} + {}^{14}N_{(a)} \rightarrow {}^{14}N_{2(g)} + 2s \qquad (8c)$$

$$2H_{(a)} + O_{(a)} \rightarrow H_2O_{(g)} + 3s \qquad (9)$$

In the scheme depicted above, NO is decomposed at reduced Pt sites to form N- and O-ad-atoms (reaction 5). Complete ammonia dehydrogenation (reaction 7) leads to the formation

of N- and H-ad-atoms, which in turn keep clean the Pt surface from O-ad-atoms via reaction 9. Eventually nitrogen formation occurs through a recombination of N-ad-atoms (reactions 8a–8c), that produces all dinitrogen isotopes with a distribution which depends on the surface concentration of ^{14}N- and ^{15}N-adatoms and can be derived on a statistical basis. At variance with the SCR pathway, this route does not result in the selective formation of only single-labeled ^{14}N^{15}N species. The concentration of ^{14}N^{15}N is limited to a maximum of 50% of total dinitrogen species, and this occurs with equal coverage of ^{14}N- and ^{15}N-ad-species.

Figure 8 shows the concentration of the ^{14}N^{15}N isotope in the % of total N$_2$ as function of time during NH$_3$-TPSR and
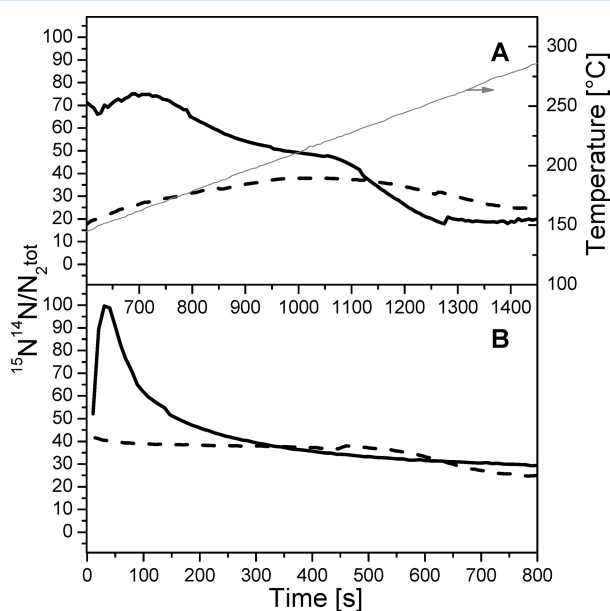

Figure 8. ^{14}N^{15}N % concentration measured during TPSR (A) and ISC (B) experiments carried out after NO$_x$ adsorption (1000 ppm ^{15}NO + O$_2$ 3% v/v in He) at 150 °C (solid lines) and at 350 °C (dashed lines).

NH$_3$-ISC experiments with nitrites and nitrates, calculated from the data of Figures 2–5. The abundance of the mixed ^{14}N^{15}N species is higher than 50% in the case of nitrites at the beginning of the experiments, up to 70% of total N$_2$ in the case of NH$_3$-TPSR (panel A) and up to 90% of total N$_2$ in the case of NH$_3$-ISC (panel B). This cannot be explained only with the statistical coupling of the N-ad-atoms formed upon adsorption/decomposition of stored ^{15}NO$_x$ and of ^{14}NH$_3$, but the occurrence of a SCR-like route involving the coupling of undissociated ^{15}NO$_x$-derived species and of ammonia fragments (e.g., NH$_2$) must also be invoked (see Otto et al.[39]):

$$^{14}NH_{2(a)} + {}^{15}NO_{(a)} \rightarrow {}^{14}N^{15}N_{(g)} + H_2O_{(a)} + s \quad (10)$$
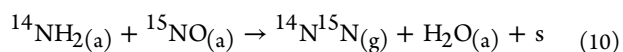
The occurrence of the SCR-like route is more favored in the case of nitrites possibly in view of the corresponding formal oxidation number of N in ammonia and nitrites (−3 and +3, respectively) which favors the formation of the NH$_x$–NO surface intermediate.[31]

As pointed out by Kondratenko and Baerns,[37] in the formation of N$_2$ over Pt the statistical coupling of N-ad-atoms and the SCR-like pathway may coexist; the contribution of these routes in the formation of dinitrogen depends on the relative

coverage by adsorbed NO and NH$_3$, and on temperature.[41] Accordingly changes in the concentration of the ^{14}N^{15}N species with time in Figure 8 are likely associated to changes in the surface concentration of NH$_3$- and nitrite- or NO-derived surface species.

The results obtained in the reduction of the stored nitrates show some distinct features. First of all the selective formation of only mixed ^{14}N^{15}N species is not possible in the NH$_3$-TPSR and NH$_3$-ISC of nitrates. In fact the formation of the double-labeled ^{14}N$_2$ isotope is expected in view of the molar ratio ^{14}NH$_3$/^{15}NO$_3^-$ = 10/6 > 1 dictated by the stoichiometry of reaction 2. Figures 4 and 5 show that all the possible N$_2$ isotopes are formed in the reduction of nitrates with ammonia, and that the phase differences of the distribution of isotopic dinitrogen species is limited. Figure 8A,B also shows that the abundance of the ^{14}N^{15}N species is still high but less that 50% of the total N$_2$ so that it is not necessary to invoke a SCR-like pathway in the case of nitrates, although it cannot be excluded. On the other hand the formation of dinitrogen isotopes originating from the self-coupling of ^{15}NO$_x$-derived species (i.e., ^{15}N$_2$) provides evidence for the occurrence of statistical coupling of the N-ad-species.

Finally, in the reduction of the gas-phase ^{15}NO with NH$_3$ in the absence of oxygen according to reaction 11:

$$6\,{}^{15}NO + 4NH_3 \rightarrow 5N_2 + 6H_2O \quad (11)$$
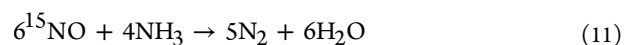
the following statistical isotope distribution is expected for the pathway based on the statistical recombination of N-ad-atoms formed by dissociation of NO and NH$_3$ at Pt sites for the feed of Figure 6: ^{14}N^{15}N/ ^{15}N$_2$/^{14}N$_2$ = 48/36/16. The isotope distribution calculated from Figure 6 at T > 200 °C where the N$_2$ selectivity is complete is ^{14}N^{15}N/ ^{15}N$_2$/^{14}N$_2 \approx$ 52/31/17. This distribution compares well with that listed above and is fully consistent with the recombination pathway of N-ad-atoms formed by decomposition of gas phase NO and NH$_3$ at Pt sites. However the SCR route, that might be involved in the formation of single-labeled N$_2$, cannot be excluded.

Formation of N$_2$O. Small and almost negligible amounts of N$_2$O have been observed during NH$_3$-TPRS and NH$_3$-ISC of nitrites (Figures 2 and 3) and of nitrates (Figures 4 and 5), respectively, while relevant quantities of N$_2$O have been detected during the NH$_3$ + NO reaction (Figure 6). Notably only the formation of labeled nitrous oxide (i.e., ^{15}N$_2$O and ^{14}N^{15}NO) has been observed during these experiments.

For comparison purposes, Figure 9 shows the N$_2$O concentration during NH$_3$-TPSR of nitrites (panel A) and during TPR of NH$_3$ and NO (panel B). The results obtained during the TPR of NH$_3$ and NO in the presence of O$_2$ (not presented previously) are also shown (panel C).

Inspection of Figure 9 shows that N$_2$O formation is poor during the reaction of stored NO$_x$ with ammonia (TPSR of nitrites, Figure 9A) but is noticeable when NO is present in the feed gas (NH$_3$ + NO reaction, Figure 9B): in this last case N$_2$O concentration is greater by 1 order of magnitude. A further increase in N$_2$O concentration is seen when oxygen is present in the feed gas (Figure 9C). These results and the fact that only labeled N$_2$O species are detected (if one neglects the small amounts of unlabeled N$_2$O observed at high temperature in Figure 9C), indicate that adsorbed ^{15}NO takes part in the formation of nitrous oxide. This is in line with literature proposals[37,40] where nitrous oxide is formed either by the coupling of two adsorbed NO molecules (reaction 12), or by
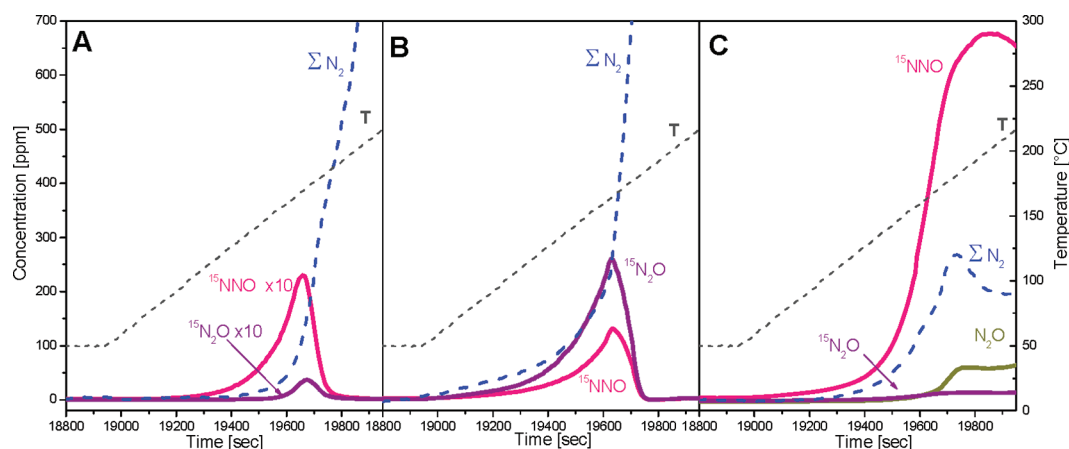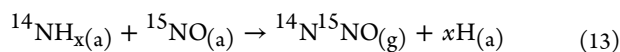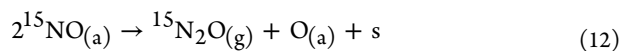
Figure 9. (A) TPSR run with NH$_3$ (1000 ppm) after ^{15}NO$_x$ adsorption at 150 °C (1000 ppm ^{15}NO + O$_2$ 3% v/v in He), (B) TPR run with NH$_3$ (660 ppm) and ^{15}NO (1000 ppm) in He, (C) TPR run with NH$_3$ (660 ppm), ^{15}NO (1000 ppm), and O$_2$ (3% v/v) in He over Pt–Ba/Al$_2$O$_3$ catalyst.

recombination of an adsorbed NO molecule with an adsorbed NH$_x$ fragment (reaction 13):

$$2^{15}NO_{(a)} \rightarrow {}^{15}N_2O_{(g)} + O_{(a)} + s \qquad (12)$$

$$^{14}NH_{x(a)} + {}^{15}NO_{(a)} \rightarrow {}^{14}N^{15}NO_{(g)} + xH_{(a)} \qquad (13)$$

These reactions are expected to occur during TPR of ^{15}NO + ^{14}NH$_3$ (Figure 6 and Figure 9B), and result in the formation of only double- and single-labeled N$_2$O species; the formation of unlabeled N$_2$O is not possible. On the other hand, during the reduction of stored nitrites ^{15}NO$_2^-$ (Figure 9A), the rate of nitrous oxide formation is limited by the low concentration of ^{15}NO-ad-species originated upon nitrite decomposition/reduction at Pt sites. Accordingly the reduction is very selective to dinitrogen.

Notably, nitrous oxide formation is strongly affected by temperature: in fact above 180 °C the N$_2$O concentration is always negligible in the absence of oxygen (Figure 9A,B). It is suggested that at high temperature NO dissociation is favored because Pt is kept in a reduced state by ammonia, and this prevents N$_2$O formation due to the lack of molecularly adsorbed NO species. Along similar lines, the nitrous oxide concentration is markedly greater in the presence of oxygen in the feed stream (compare Figure 9B,C) because NO dissociation is prevented over the oxygen-covered Pt surface and this increases the concentration of NO ad-species.

However, under reducing conditions the possibility that N$_2$O is reduced to N$_2$ cannot be excluded. In this light the decrease in N$_2$O concentration which is seen upon increasing the temperature in the absence of oxygen (Figures 9, panels A and B) might be due to the reduction of N$_2$O to give N$_2$.[41] This route may contribute only to the formation of single and double-labeled N$_2$ molecules in the experiments of Figure 9 panel A (i.e., Figure 2) and panel B (i.e., Figure 6) but not in the formation of unlabeled N$_2$ because of the lack of ^{14}N$_2$O and because the reduction of N$_2$O does not involve the cleavage of the N–N bond.[41]

It is worth noting that the presence of oxygen in the feed changes the nitrous oxide isotopic distribution during the TPR of NH$_3$+NO (compare Figure 9B,C). In fact while in the absence of oxygen the double-labeled nitrous oxide isotope (^{15}N$_2$O) prevails over the single-labeled species (^{14}N^{15}NO)

(Figure 9B), in the presence of oxygen (Figure 9C) the formation of the double-labeled nitrous oxide molecule is negligible. Indeed the abundance of adsorbed oxygen drives reaction 12 from right to left so that the formation of ^{15}N$_2$O is less favored. On the other hand, since the overall nitrous oxide concentration is greater in the presence of oxygen, it turns out that reaction 13 must be favored by O$_2$ concentration. As a matter of fact, it was also reported that the presence of adsorbed oxygen species favors ammonia activation yielding reactive NH$_x$ adsorbed intermediates.[38] This may result in the presence of a pool of unlabeled NH$_x$ fragments whose reaction with molecularly adsorbed ^{15}NO results in the formation of single-labeled nitrous oxide molecules (reaction 13), as indeed observed. Notably, nitrous oxide formation due to ammonia oxidation

$$2^{14}NH_{x(a)} + (x + 1)O_{(a)} \rightarrow {}^{14}N_2O_{(g)} + xH_2O \qquad (14)$$
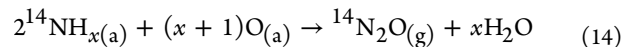
is limited compared to reaction 13 during the TPR of NH$_3$ + NO in the presence of oxygen (Figure 9C) as pointed out by the relatively small amounts of unlabeled N$_2$O as compared to ^{15}N^{14}NO.

Finally, it is noted that small amounts of N$_2$O are detected at low temperature during the TPSR of stored nitrites (Figures 2 and 3), whereas the reaction is very selective to nitrogen in the case of nitrates (Figures 4 and 5). As shown by dedicated TPD and H$_2$-TPSR experiments carried out over the stored nitrites and nitrates (not reported for the sake of brevity), the reduction/decomposition of nitrites onto the Pt sites occurs at lower temperatures than that of nitrates. This may lead, upon nitrite reduction, to the formation of NO-related intermediate ad-species that at low temperatures are involved in nitrous oxide formation. In fact these species are not readily decomposed to N- and O-ad-atoms due to the poor reducing capability of ammonia. At variance, the reduction/decomposition of nitrates is observed at slightly higher temperatures, and this would favor the decomposition of the NO-related adsorbed intermediates.

■ CONCLUSIONS

In this paper mechanistic aspects involved in the formation of N$_2$ and N$_2$O during the reduction of NO$_x$ stored over a model PtBa/Al$_2$O$_3$ NSR catalyst have been investigated by means of isotopic labeling experiments. The combined use of MS,

UV−vis, and GC analysis has been adopted to allow a complete quantitative analysis of the reaction products.

The reduction of stored labeled NO_x species (nitrites and nitrates) with unlabeled NH_3 leads to the selective formation of N_2, since only very small amounts of nitrous oxide have been observed in the reduction of nitrites only. The observed N_2 isotopic distribution includes all possible N_2 isotopes, that is, $^{15}N_2$, $^{14}N_2$, and the mixed $^{15}N^{14}N$ species. On the basis of the pathway suggested for NO and NH_3 reaction on Pt-based catalysts, it has been found that the observed product distribution can be explained on the basis of the statistical coupling of ^{15}N- and ^{14}N-adatoms originated upon NH_3 and NO_x decomposition on Pt. However the simultaneous occurrence of a SCR-like pathway, involving the formation and decomposition of a NH_x-NO intermediate originating from ammonia and NO_x, and leading to the selective formation of the mixed $^{15}N^{14}N$ species is also likely. In fact at the early stages of the reduction of stored labeled nitrites with unlabeled ammonia the reduction process is selective toward the formation of the mixed $^{15}N^{14}N$ isotope, suggesting the occurrence of a SCR-like pathway.

Isotopic labeling experiments also provide indications on the pathways involved in the formation of N_2O. This species is formed in very limited amounts during the reduction by ammonia of stored NOx species (nitrites and nitrates); much higher quantities have been observed during the reduction of gaseous ^{15}NO with NH_3. Since no formation of unlabeled nitrous oxide has been observed, the participation of ^{15}NO is necessary for the formation of nitrous oxide. In line with literature proposals, it has been suggested that nitrous oxide formation involves (on the Pt sites) either the coupling of two adsorbed NO molecules or the recombination of an adsorbed NO molecule with an adsorbed NH_x fragment. Accordingly, N_2O formation is greatly enhanced in the presence of gas-phase NO.

Temperature also drives the selectivity to nitrous oxide. This product is favored at low temperature and is likely related to the oxidation state of Pt: at high temperatures Pt is kept in a reduced state by ammonia, and this would favor NO dissociation on the Pt sites thus preventing N_2O formation. Besides, N_2O could be reduced to N_2. The presence of oxygen in the feed stream favors N_2O formation, since it increases the concentration of molecularly adsorbed NO species and inhibits N_2O reduction. The route involving the coupling of NO-ad-species is however inhibited by the presence of oxygen, and hence nitrous oxide formation involves adsorbed NO and NH_x fragments.

■ **AUTHOR INFORMATION**

Corresponding Author

*Tel.: +39 02 2399 3272. Fax: +39 02 7063 8173. E-mail: luca.lietti@polimi.it.

Notes

The authors declare no competing financial interest.

■ **REFERENCES**

(1) Johnson, T. V. Diesel emission review. *SAE Int. J. Eng.* **2011**, *4*, 143.

(2) Granger, P.; Parvulescu, V. I. Catalytic NO_x abatement systems for mobile sources: From three-way to lean burn after-treatment technologies. *Chem. Rev.* **2011**, *111*, 3155.

(3) Baiker, R. S. NO_x Storage-reduction catalysis: From mechanism and materials properties to storage-reduction performance. *Chem. Rev.* **2009**, *109*, 4054.

(4) Takahashi, N.; Shinjoh, H.; Iijima, T.; Suzuki, T.; Yamazaki, K.; Yokota, K.; Suzuki, H.; Miyoshi, N.; Matsumoto, S.; Tanizawa, T.; Tanaka, T.; Tateishi, S.; Kasahara, K. The new concept 3-way catalyst for automotive lean-burn engine: NO_x storage and reduction catalyst. *Catal. Today* **1996**, *27*, 63.

(5) Epling, W.; Campbell, L.; Yezerets, A.; Currier, N.; Parks, J. Overview of the fundamental reactions and degradation mechanism of NO_x storage/reduction catalysts. *Catal. Rev. Sci. Eng.* **2004**, *46*, 163.

(6) Miyoshi, N.; Matsumoto, S.; Katoh, K.; Tanaka, T.; Harada, J.; Takahashi, N.; Yokota, K.; Sugiura, M.; Kasahara, K. Development of new concept three-way catalyst for automotive lean-burn engines. *SAE Tech. Pap.* **1995**, 950809.

(7) Johnson, T. Diesel engine emissions and their control. *Platinum Metals Rev.* **2008**, *52*, 23.

(8) Castoldi, L.; Bonzi, R.; Lietti, L.; Forzatti, P. Catalytic behaviour of hybrid LNT/SCR systems: Reactivity and in situ FTIR study. *J. Catal.* **2011**, *1*, 128.

(9) Toops, T. J.; Smith, D. B; Partridge, W. P. NO_x adsorption on Pt/K/Al$_2$O$_3$. *Catal.Today* **2008**, *114*, 112.

(10) Konsolakis, M.; Yentekakis, I. V. Strong promotional effects of Li, K, Rb, and Cs on the Pt-catalysed reduction of NO by propene. *Appl. Catal. B, Environ.* **2001**, *29*, 103.

(11) Nova, I.; Lietti, L.; Castoldi, L.; Tronconi, E.; Forzatti, P. New insights in the NO_x reduction mechanism with H$_2$ over Pt-Ba/γ-Al$_2$O$_3$ lean NO_x trap catalysts under near-isothermal conditions. *J. Catal.* **2006**, *239*, 244.

(12) Breen, J. P.; Burch, R.; Fontaine-Gautrelet, C.; Hardacre, C.; Rioche, C. Insight into the key aspects of the regeneration process in the NO_x storage reduction (NSR) reaction probed using fast transient kinetics coupled with isotopically labelled ^{15}NO over Pt and Rh-containing Ba/Al$_2$O$_3$ catalysts. *Appl. Catal. B, Environ.* **2008**, *81*, 150.

(13) Lietti, L.; Nova, I.; Forzatti, P. Role of ammonia in the reduction by hydrogen of NO_x stored over Pt-Ba/Al$_2$O$_3$ lean NO_x trap catalysts. *J. Catal.* **2008**, *257*, 270.

(14) Cumaranatunge, L.; Mulla, S. S.; Yezerets, A; Currier, N. W.; Delgass, W. N.; Ribeiro, F. H. Ammonia is a hydrogen carrier in the regeneration of Pt/BaO/Al$_2$O$_3$ NO_x traps with H$_2$. *J. Catal.* **2007**, *246*, 29.

(15) Bhatia, D.; Harold, M. P.; Balakotaiah, V. Modeling the effect of Pt dispersion and temperature during anaerobic regeneration of a lean NO_x trap catalyst. *Catal. Today* **2010**, *151*, 314.

(16) Castoldi, L.; Nova, I.; Lietti, L.; Tronconi, E.; Forzatti, P. The NO_x reduction mechanism by H$_2$ under near isothermal conditions over Pt-Ba/Al$_2$O$_3$ lean NO_x trap systems. *Top. Catal.* **2007**, *42−43*, 189.

(17) Nova, I.; Lietti, L.; Forzatti, P. Mechanistic aspects of the reduction of stored NO_x over Pt-Ba/Al$_2$O$_3$ lean NO_x trap systems. *Catal. Today* **2008**, *136*, 128.

(18) Forzatti, P.; Lietti, L.; Nova, I. On board catalytic NO_x control: Mechanistic aspects of the regeneration of lean NO_x traps with H$_2$. *Energy. Environ. Sci.* **2008**, *1*, 236.

(19) Partridge, W. P.; Choi, J. S. NH_3 formation and utilization in regeneration of Pt/Ba/Al$_2$O$_3$ NO_x storage-reduction catalyst with H$_2$. *Appl. Catal. B Environ.* **2009**, *91*, 144.

(20) Forzatti, P; Lietti, L.; Gabrielli, N. A kinetic study of the reduction of NO_x stored on Pt-Ba/Al$_2$O$_3$ catalyst. *Appl. Catal. B, Environ.* **2010**, *99*, 145.

(21) Mulla, S. S.; Chaugule, S. S.; Yezerets, A.; Currier, N. W.; Delgass, W. N.; Ribeiro, F. H. Regeneration mechanism of Pt/BaO/Al$_2$O$_3$ lean NO_x trap catalyst with H$_2$. *Catal. Today.* **2008**, *136*, 136.

(22) Castoldi, L.; Nova, I.; Lietti, L.; Forzatti, P. Study of the effect of Ba loading for catalytic activity of Pt-Ba/Al$_2$O$_3$ model catalysts. *Catal. Today* **2004**, *96*, 43.

(23) Miyoshi, N.; Tanizawa, T.; Kasahara, K.; Tateishi, S. European Patent application 0 669 157 A1, 1995.

(24) Nova, I.; Castoldi, L; Prinetto, F.; Dal Santo, V.; Lietti, L.; Tronconi, E.; Forzatti, P.; Ghiotti, G.; Psaro, R.; Recchia, S. NO_x adsorption study over Pt−Ba/alumina catalysts: FT−IR and reactivity study. *Top. Catal.* **2004**, *30/31*, 181.

(25) Prinetto, F.; Ghiotti, G.; Nova, I.; Castoldi, L.; Lietti, L.; tronconi, E.; Forzatti, P. In situ Ft−IR and reactivity study of NO_x storage over Pt−Ba/γ-Al_2O_3 catalysts. *Phys. Chem. Chem. Phys.* **2003**, *5*, 4428.

(26) Nova, I.; Castoldi, L.; Lietti, L.; Tronconi, E.; Forzatti, P.; Prinetto, F.; Ghiotti, G. NO_x adsorption study over Pt-Ba/alumina catalysts: FT-IR and pulse experiments. *J. Catal.* **2004**, *222*, 377.

(27) Lietti, L.; Daturi, M.; Blasin-Aubé, V.; Ghiotti, G.; Prinetto, F.; Forzatti, P. Relevance of nitrite route in the NO_x adsorption mechanism over Pt-Ba/Al_2O_3, NSR catalysts investigated by FT-IR operando spectroscopy. *Chem Catal. Chem.* **2012**, *4*, 55.

(28) Ozkan, U. S; Cai, Y.; Kumthehkar, M. W. Investigation of the reaction pathways in selective catalytic reduction of NO with NH_3 over V_2O_5 catalysts: Isotopic labeling studies using $^{18}O_2$, $^{15}NH_3$, ^{15}NO, and $^{15}N^{18}O$. *J. Catal.* **1994**, *149*, 390.

(29) Chen, H.; Sun, Q.; Wen, B.; Yeom, Y.; Weiz, E.; Sachtler, W. M. Reduction over zeolite-based catalysts of nitrogen oxides in emissions containing excess oxygen: Unraveling the reaction mechanism. *Catal. Today* **2004**, *96*, 1.

(30) Janssen, F J J. G.; Van Den Kerkhof, F. M. G.; Bosh, H.; Ross, J. R. H. Mechanism of the reaction of nitric oxide, ammonia and oxygen over vanadia catalysts 1. The role of oxygen studied by way of isotopic transient under dilute conditions. *J. Phys. Chem.* **1987**, *91*, 6633.

(31) Busca, G.; Lietti, L.; Ramis, G.; Berti, F. Chemical and mechanistic aspects of the selective catalytic reduction of NO_x by ammonia over oxide catalysts: A review. *Appl. Catal. B. Environ.* **1998**, *18*, 1.

(32) Yeom, Y.; Li, M; Savara, A.; Sachtler, W; Weitz, E. An overview of the mechanisms of NO_x reduction with oxygenates over zeolite and γ-Al_2O_3 catalysts. *Catal. Today* **2008**, *136*, 55.

(33) Kumar, A.; Harold, M. P.; Balakotaiah, V. Isotopic studies of NO_x storage and reduction on Pt/BaO/Al_2O_3 catalyst using temporal analysis of products. *J. Catal.* **2010**, *270*, 214.

(34) Kondraratenko, V. A.; Baerns, M. Mechanistic insights into the formation of N_2O and N_2 in NO reduction by NH_3 over a polycrystalline platinum catalyst. *Appl. Catal. B. Environ.* **2007**, *70*, 111.

(35) Van Tol, M. F. H.; Siera, J.; Cobden, P. D.; Nieuwenhuys, B. E. Oscillatory behavior of the reduction of NO by H_2 over Rh. *Surf. Sci.* **1992**, *274*, 63.

(36) Nova, I.; Castoldi, L.; Lietti, L.; Tronconi, E.; Forzatti, P.; Prinetto, F.; Ghiotti, G. The Pt−Ba interaction in lean NO_x trap systems. *SAE Tech. Pap.* **2005**, 1085.

(37) Nova, I.; Castoldi, L.; Lietti, L.; Tronconi, E.; Forzatti, P. A low temperature pathway operating the reduction of stored nitrates in Pt-Ba/Al_2O_3 lean NO_x trap systems. *SAE Tech. Pap.* **2006**, 1368.

(38) Perez-Ramirez, J.; Kondratenko, E. V.; Kondratenko, V. A.; Baerns, M. Selectivity-directing factors of ammonia oxidation over PGM gauzes in the temporal analysis of products reactor: Secondary interactions of NH_3 and NO. *J. Catal.* **2005**, *229*, 303.

(39) Otto, K.; Shelef, M.; Kummer, J. T. Studies of surface reactions of nitric oxide by nitrogen-15 isotope labeling. I. Reaction between nitric oxide and ammonia over supported platinum at 200−250°. *J. Phys. Chem.* **1970**, *74*, 2690.

(40) Burch, R.; Shestov, A. A.; Sullivan, J. A. A steady-state isotopic transient kinetic analysis of the NO/O_2/H_2 reaction over Pt/SiO_2 catalysts. *J. Catal.* **1999**, *188*, 69.

(41) Cant, N. W; Chambers, D. C.; Liu, I. O. Y. The reduction of $^{15}N^{14}NO$ by CO and by H_2 over Rh/SiO_2: A test of a mechanistic proposal. *J. Catal.* **2011**, *278*, 162.

7605

dx.doi.org/10.1021/ie2021976 | *Ind. Eng. Chem. Res.* 2012, 51, 7597−7605